PARASITE GENETICS

Large-scale RNAi screening uncovers therapeutic targets in the parasite *Schistosoma mansoni*

Jipeng Wang[1]*, Carlos Paz[1]*, Gilda Padalino[2], Avril Coghlan[3], Zhigang Lu[3], Irina Gradinaru[1], Julie N. R. Collins[1], Matthew Berriman[3], Karl F. Hoffmann[2], James J. Collins III[1]†

Schistosome parasites kill 250,000 people every year. Treatment of schistosomiasis relies on the drug praziquantel. Unfortunately, a scarcity of molecular tools has hindered the discovery of new drug targets. Here, we describe a large-scale RNA interference (RNAi) screen in adult *Schistosoma mansoni* that examined the function of 2216 genes. We identified 261 genes with phenotypes affecting neuromuscular function, tissue integrity, stem cell maintenance, and parasite survival. Leveraging these data, we prioritized compounds with activity against the parasites and uncovered a pair of protein kinases (TAO and STK25) that cooperate to maintain muscle-specific messenger RNA transcription. Loss of either of these kinases results in paralysis and worm death in a mammalian host. These studies may help expedite therapeutic development and invigorate studies of these neglected parasites.

S tudies of gene function in intramammalian schistosome parasites have been limited to relatively small numbers of genes (*1*). Therefore, we developed a large-scale RNA interference (RNAi) screening platform on adult schistosomes that prioritized a list of 2320 of the worm's ~10,000 protein-coding genes (fig. S1A and table S1). We generated double-stranded RNAs (dsRNAs) and treated adult male and female pairs with dsRNA over the course of a 30-day experiment (Fig. 1A). After filtering genes that either did not amplify by polymerase chain reaction or failed to generate sufficient concentrations of dsRNA, a total of 2216 genes were screened (table S1).

Schistosomes live in the veins surrounding the host intestines and attach to the vascular endothelium to avoid being swept away in the blood and trapped in host organs. Under in vitro culture conditions, healthy parasites attach to the substrate with a combination of their oral and ventral suckers (movie S1). We thus reasoned that substrate attachment would be a useful quantitative metric to define RNAi treatments that affect parasite vitality and to predict in vivo survival. Therefore, we monitored parasites for 30 days to identify substrate attachment and other visible defects.

Schistosomes possess adult somatic stem cells (neoblasts) that rejuvenate parasite tissues, including the intestine and tegument (skin) (*2*, *3*). The parasites also contain large numbers of proliferative germline stem cells (GSCs) in their reproductive organs (*2*) that are essential for producing eggs, the central drivers of parasite-induced pathology in vivo

(*4*). Therefore, we monitored the maintenance of neoblasts and GSCs by labeling parasites with the thymidine analog ethynyl deoxyuridine (EdU) before the conclusion of the experiment (Fig. 1A). Because of the variable rate at which the reproductive organs of female worms degenerate during in vitro culture (*5*), stem cell proliferation was only monitored in male worms. For genes with RNAi phenotypes uncovered during our screen, we confirmed gene identity by sequencing and mitigated potential off-target effects by designing an additional dsRNA targeting a nonoverlapping gene region or by examining sequence identity of hits with other *Schistosoma mansoni* genes (fig. S1). These studies identified 195 genes with fully penetrant attachment phenotypes, of which 121 possessed phenotypes in addition to attachment, including tissue and intestinal edema (36 genes), head (26) and/or tegument (78) degeneration, muscular hypercontraction (6), and death (36) (Fig. 1B and table S2). RNAi of an additional 66 genes resulted in stem cell maintenance defects but caused no other visible phenotypes (e.g., attachment), suggesting an essential role for stem cell maintenance (fig. S2 and table S3). We cannot rule out the possibility of false negatives among the genes with no phenotype and encourage greater scrutiny of such genes by alternate knockdown approaches or analysis of different phenotypic readouts.

Of the 66 genes required for stem cell survival, RNAi of over 90% (60 of 66) led to defects in the maintenance of both proliferative cells in the male testes and neoblasts (fig. S2). However, for a minority of genes, this maintenance defect appeared to be specific to either proliferative cells in the testes or neoblasts (fig. S2). Gene Ontology enrichment analysis identified genes important for protein translation, including gene products involved in ribosomal structure, tRNA amino-

acylation, and ribosomal RNA (rRNA) processing as putative regulators of proliferative cell maintenance (fig. S3A). Although this could reflect an enhanced sensitivity of actively proliferating cells to alterations in protein translation, studies have highlighted "nonhousekeeping" roles for translational regulators in controlling stem cell function (*6*).

Of the 195 genes essential for parasite attachment, a large fraction share sequence similarity with other organisms, including other medically relevant schistosome species (table S4). Additionally, most genes with an attachment phenotype (172 of 195 genes; 88%) possess a close homolog from *Caenorhabditis elegans* or *Drosophila melanogaster* that likewise has a loss-of-function phenotype (table S5). Gene Ontology analyses of genes with attachment phenotypes further revealed that the dominant group of enriched genes were those encoding components necessary for protein turnover via the ubiquitin-proteasome system (UPS) (fig. S3B). Proteolysis is important for larval and adult viability in vitro (*7*, *8*), and our data identified that key components from virtually every arm of the UPS were required for adult parasite vitality during in vitro culture (fig. S4A). Indeed, RNAi of nearly all UPS components resulted in extensive tissue degeneration and in some cases adult parasite death (fig. S4, B and C).

To determine if any genes associated with attachment phenotypes encoded proteins targeted by existing pharmacological agents, we searched the literature and the ChEMBL database (table S6) (*9*). This analysis uncovered 205 compounds potentially targeting 49 *S. mansoni* proteins. We selected 14 of these compounds (table S7) and examined the activities of these compounds on worms cultured in vitro either by automated worm movement tracking or on the basis of parasite attachment. More than half of the compounds tested (8 of 14) on worms at 10 μM reduced parasite movement by >75%, and half of the compounds (7 of 14) caused fully penetrant substrate attachment defects by day 7 posttreatment (Fig. 2, A and B, and movie S2). Similarly, seven of these compounds affected the movement of postinfective larvae (schistosomula), suggesting activity against multiple life cycle stages (table S8).

Among the compounds that emerged from these studies was simvastatin, a 3-hydroxy-3-methylglutaryl coenzyme A reductase inhibitor with known effects on parasites both in vitro and in vivo (*10*). The proteasome inhibitor ixazomib affected both schistosome movement (Fig. 2A) and attachment (Fig. 2B), mirroring results in a recent report of the proteasome inhibitor bortezomib (*7*). However, the most potent effects on adult parasites were observed with CB-5083 and NMS-873, which inhibit the UPS component p97 by either competing with adenosine triphosphate

[1]Department of Pharmacology, UT Southwestern Medical Center, Dallas, TX 75390, USA. [2]Institute of Biological, Environmental and Rural Sciences (IBERS), Aberystwyth University, Aberystwyth, Wales, UK. [3]Wellcome Sanger Institute, Wellcome Genome Campus, Hinxton, Cambridge CB10 1SA, UK.

*These authors contributed equally to this work.
†Corresponding author. Email: jamesj.collins@utsouthwestern.edu

(ATP) (*11*) or binding to an allosteric site (*12*), respectively (fig. S5A). Similar to the death observed after long-term *p97* RNAi treatment (Fig. 1B), both p97 inhibitors led to death in vitro (movie S3). Despite their distinct biochemical mechanisms of action, we noted similar deformations in the structure of the parasite tegument after treatment with either CB-5083 or NMS-873, suggesting that these compounds have similar pharmacological effects on the parasite (Fig. 2C).

We then assessed if NMS-873 and CB-5083 affected UPS function by measuring the accumulation of ubiquitinated proteins using an antibody that recognizes Lys^{48} (K48) polyubiquitinated proteins marked for proteasome-mediated destruction (*13*). We observed the accumulation of polyubiquitinated proteins after RNAi of *p97* and after treatment of schistosomes with either CB-5083 or NMS-873 (fig. S5B). Consistent with CB-5083 or NMS-873 acting via *p97* inhibition to blunt protein degradation, we found that *p97* RNAi treatment together with low concentrations of either drug led to additive increases in polyubiquitinated protein accumulation (fig. S5C). We also observed accumulation of polyubiquitinated proteins after either RNAi of *proteasome subunit beta type-2* or treatment with ixazomib (fig. S5D). These effects on the degradation of ubiquitinated proteins appeared to be specific to inhibition of UPS function

rather than a nonspecific effect due to reduced worm vitality (fig. S5D).

We then depleted UPS components using RNAi and surgically transplanted these worms into the mesenteric veins of recipient mice (fig. S6A), and we measured parasite egg deposition in host tissues and parasite survival. After hepatic portal perfusion, we recovered about 55% of transplanted control RNAi-treated worms (Fig. 2D and fig. S6B), and these parasites established patent infections, depositing large number of eggs into the livers of recipient mice (Fig. 2E and fig. S6, C and D). By contrast, we failed to recover parasites after hepatic portal perfusion of mice receiving *p97* (Fig. 2D) or *proteasome subunit beta type-2* (fig. S6B). As a consequence, the livers in these mice were devoid of eggs, and we observed no signs of egg-induced granulomata (Fig. 2E and fig. S6, C and D). We also observed RNAi-treated parasites at various stages of infiltration by host immune cells (fig. S6, E and F). This suggests that these parasites are unable to remain in the portal vasculature and are cleared via the liver by the immune system. Taken together, these data highlight the essentiality and druggability of the schistosome UPS.

Another group of potentially druggable targets to emerge from our RNAi screen were protein kinases, 19 of which led to defects in either parasite attachment or stem cell maintenance. RNAi of two STE20 serine-threonine

kinases, *tao* and *stk25*, which are homologs of the human TAO1/2/3 and STK25/YSK1 protein kinases, respectively, led to rapid detachment from the substrate (fig. S7A) and a concomitant posterior paralysis and hypercontraction of the body, such that the parasites took on a distinctive "banana"-shaped morphology (Fig. 3A, fig. S7B, and movie S4). Aside from RNAi of *stk25* and *tao*, this banana-shaped phenotype of worms was distinctive, as it was only observed after RNAi of a CCM3/PDCD10 homolog (Smp_031950), a known heterodimerization partner with the mammalian STK25 kinase (*14*). We failed to observe death of either *stk25*- or *tao*-depleted parasites during in vitro culture. However, after surgical transplantation, we noted a reduction in the recovery of *tao* or *stk25* RNAi-treated parasites from recipient mice, and these recipient mice displayed few signs of egg-induced granulomata formation (Fig. 3, B and C, and fig. S7, C and D). Thus, both *tao* and *stk25* appear to be essential for schistosome survival in vivo.

Given the distinct and specific nature of the *stk25*- and *tao*-associated banana phenotype, we reasoned that these kinases may act in concert to mediate signaling processes in the worm. The *Drosophila* STK25 ortholog (GCK3) is a substrate of TAO, and these proteins function in a signaling cascade essential for tracheal development (*15*). Likewise, we observed that recombinant *S. mansoni* STK25
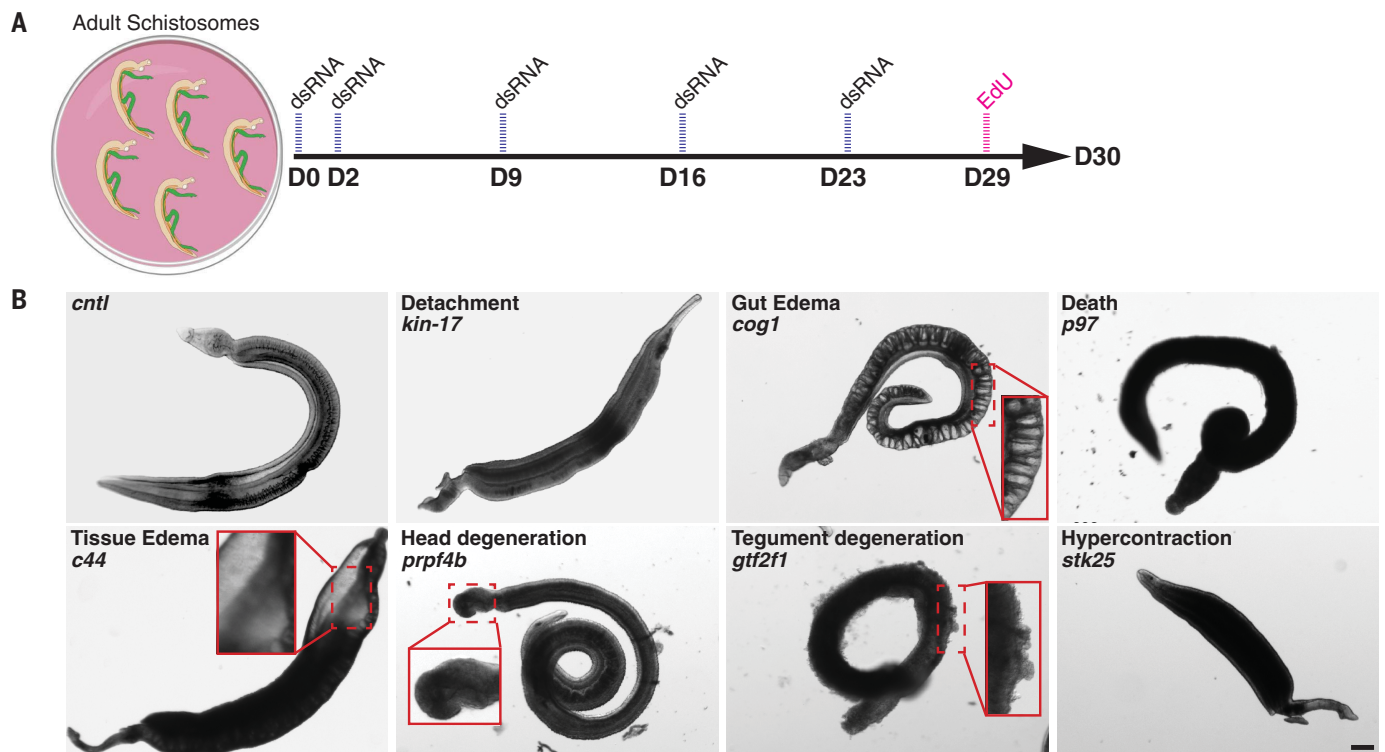

Fig. 1. Summary of RNAi phenotypes. (**A**) RNAi treatment regimen. Parasites were monitored for visible abnormalities, and at day 29 EdU was added to medium to label proliferative cells. (**B**) Categories of RNAi phenotypes observed. *kin-17* (Smp_023250), *cog1* (Smp_132980), *p97* (Smp_018240), *c44* (Smp_136260), *prpf4b* (Smp_068960), *gtf2f1* (Smp_088460), *stk25* (Smp_096640). Scale bar, 100 μm.
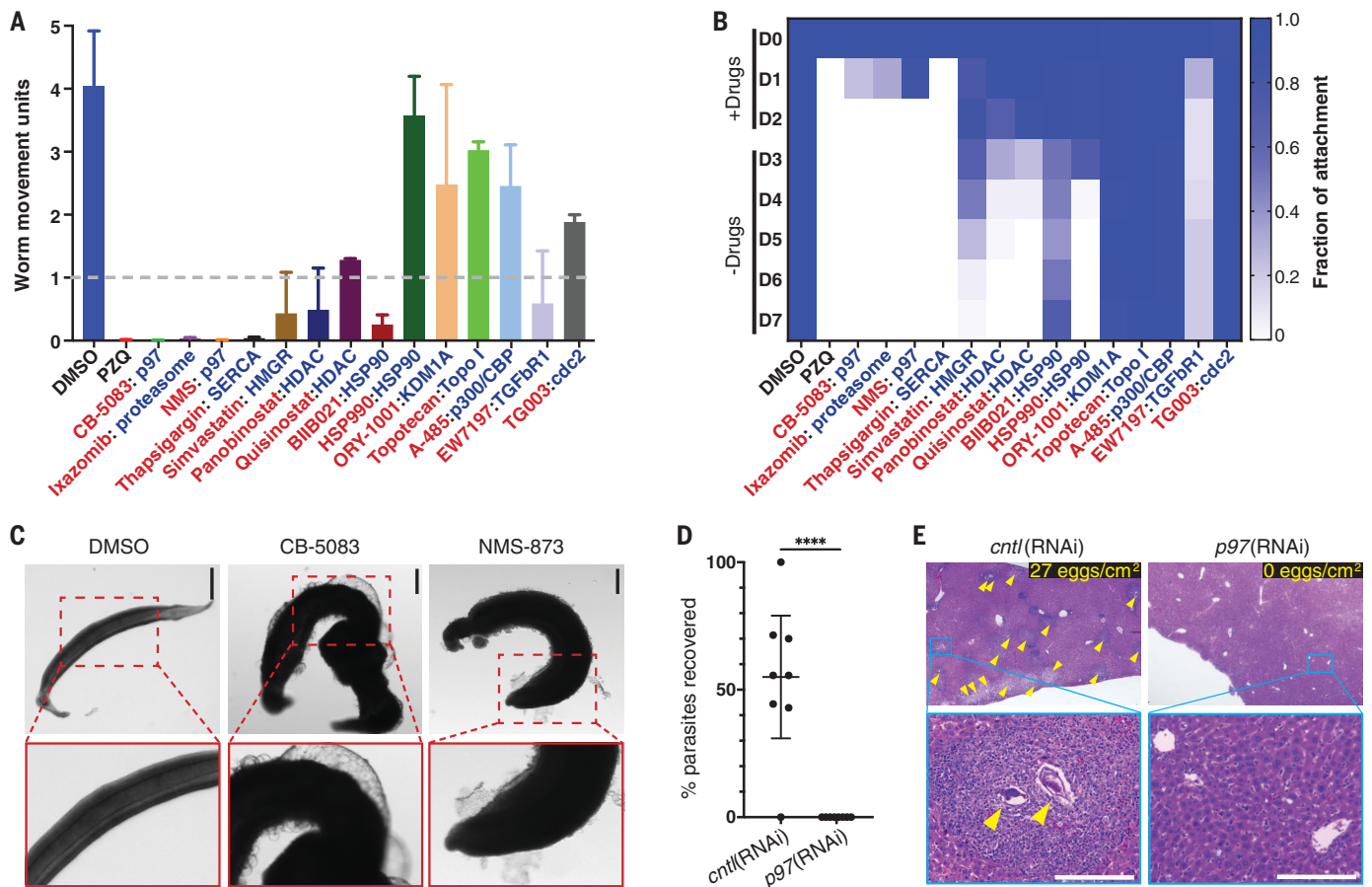
Fig. 2. Compounds prioritized from RNAi studies have effects on schistosomes in vitro. (**A**) Effects on worm motility of compounds (red text) at 10 μM for 72 hours predicted to target schistosome proteins (blue text) essential for parasite attachment. n = 12 worm pairs, evaluated in three biological replicates. Data are means ± SD. Dashed line, threshold for 75% reduction in motility. DMSO, dimethyl sulfoxide (control). (**B**) Heat map showing time course for the fraction of male worms attached to the substrate after treatment with compounds for 72 hours as in (A). Three biological replicates were performed. (**C**) Effects of CB-5083 or NMS-873 (10 μM, 72 hours) treatment on male parasites. (**D**) Percent recovery of *p97*(RNAi) or control RNAi [*cntl*(RNAi)] male parasites surgically transplanted into mice. n = 8 transplants for each group. ****P < 0.0001, t test. Data are means ± 95% confidence intervals (CIs). (**E**) Hematoxylin and eosin staining of livers from mice receiving control or *p97*(RNAi) parasites. Yellow arrowheads indicate egg-induced granulomata. (Top right) Counts of eggs per square centimeter of liver section are shown (n = 3 livers). Scale bars, 100 μm [(C) and (E)].

(SmSTK25) could serve as a substrate for the *S. mansoni* TAO (SmTAO) in an in vitro kinase assay (fig. S8, A and B). The human STK25 is activated by phosphorylation of a conserved threonine residue within its activation loop (*16*). By mass spectrometry, we observed that this conserved threonine (T) within the predicted SmSTK25 activation loop (T173) was phosphorylated after incubation of recombinant SmTAO with catalytically inactive SmSTK25 (fig. S8, C and D). Using an antibody that recognizes activation loop phosphorylation in STK25 orthologs (*16*), Western blotting revealed SmSTK25 T173 autophosphorylation after an in vitro kinase reaction; this signal was abrogated in controls lacking ATP and when the SmSTK25 catalytic K48 residue was mutated to arginine (R) (Fig. 3D and fig. S8E). Consistent with our mass spectrometry results, we detected robust phosphorylation of T173 when recombinant SmTAO

was incubated with kinase-dead SmSTK25 (kdSmSTK25) (Fig. 3D), suggesting that SmTAO can phosphorylate a key residue for the activation of the mammalian STK25.

We reasoned that the schistosome TAO and STK25 might be acting in a signaling module to mediate critical processes in the parasite. To define these processes, we performed transcriptional profiling on RNAi-treated parasites just before observing detachment and hypercontraction (day 6 and day 9 for *tao* and *stk25* RNAi treatments, respectively) (fig. S9, A and B). We found that expression levels of differentially regulated genes after RNAi with either *tao* or *stk25* were correlated (Fig. 3E) and that more than half of these differentially regulated genes were common in both datasets (fig. S9C and table S9). Notably, RNAi of either *tao* or *stk25* was specific and did not affect expression of the other kinase gene of this pair (Fig. 3, E and F).

By examining the tissue-specific expression of differentially regulated genes on an adult schistosome single-cell expression atlas using cells from schistosome somatic tissues (*17*), we found that roughly 40% (51 of 129) of the most–down-regulated genes after *tao* and *stk25* RNAi were specific markers of parasite muscle cells (fig. S10, A to C, and table S9). Indeed, nearly half of all mRNAs specifically enriched in muscle cells (60 of 135) from this single-cell atlas, including key muscle contractile proteins, were down-regulated after RNAi of *tao* and *stk25* (Fig. 3F; fig. S10, B and D; and table S10). These transcriptional effects appeared to be largely specific to parasite muscles (Fig. 3F, fig. S10B, and table S10).

In principle, loss of muscle-specific mRNAs could be due to either loss of muscle cells or down-regulation of muscle-specific mRNAs. We therefore labeled F-actin in schistosome muscle fibers with phalloidin and performed
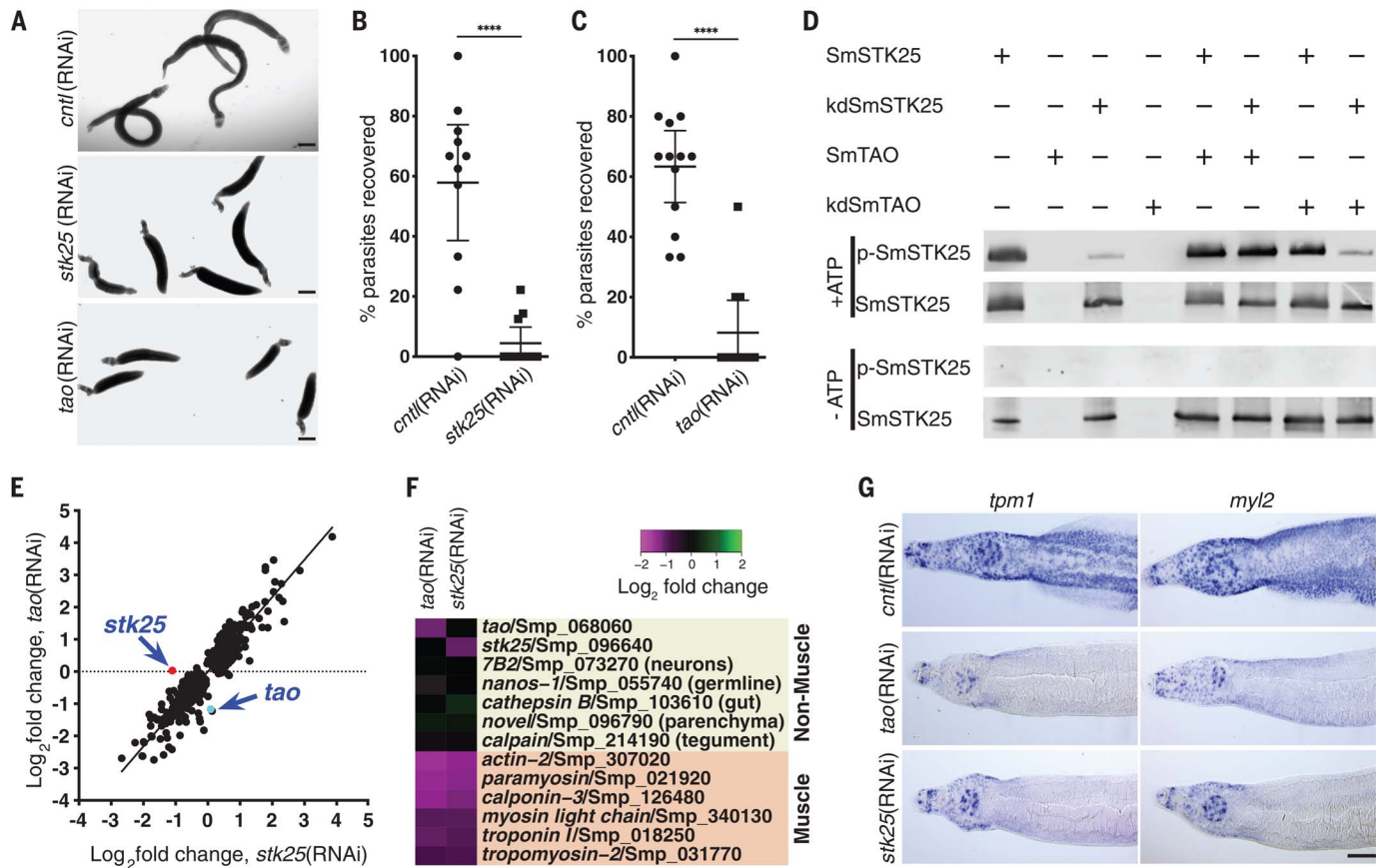
Fig. 3. The protein kinases SmSTK25 and SmTAO are essential to maintain muscular function. (**A**) RNAi of *stk25* or *tao* causes parasite hypercontraction. (**B** and **C**) Percent recovery of *stk25*(RNAi), *tao*(RNAi), or control(RNAi) male parasites surgically transplanted into mice. *n* ≥ 11 transplants for each group. ****$P < 0.0001$, *t* test. Data are means ± 95% CIs. (**D**) Western blot to detect phospho-T173 (p-SmSTK25) or total SmSTK25 after an in vitro kinase reaction with or without ATP. Data represent results of two experiments. (**E**) Scatter plot showing the relationship between the differentially expressed genes [*P*(adjusted) < 0.001; Benjamini-Hochberg–corrected Wald test] after *stk25* or *tao* RNAi treatment (*r* = 0.9, *P* < 0.0001; Pearson correlation). (**F**) Heat map showing expression of tissue-specific transcripts after RNAi of *tao* or *stk25*. (**G**) In situ hybridization for *tropomyosin 1* (*tpm1*; Smp_340760) and a myosin light chain (*myl2*; Smp_132670) after RNAi at day 13. Scale bars, 500 µm (A) or 100 µm (G).

in situ hybridization to detect muscle-specific mRNAs. RNAi-treated parasites exhibited a reduction in the expression of mRNAs encoding the contractile proteins tropomyosin 1 and myosin light chain by in situ hybridization (Fig. 3G) but no qualitative defects in phalloidin staining of body wall muscles (fig. S11). Thus, it appears that these kinases are required to maintain the transcription of many muscle-specific mRNAs in intact muscle cells. The heads of *tao* and *stk25* RNAi parasites retained their capacity for movement (movie S4) and partially maintained the expression of muscle-specific mRNAs (Fig. 3G). Thus, there appears to be a relationship between the maintenance of muscle-specific mRNA expression and locomotion.

Taken in their entirety, our data suggest that STK25 and TAO kinases cooperate in the schistosome to mediate signaling essential for sustaining the transcription of muscle-specific mRNAs. As a consequence, loss of either SmSTK25 or SmTAO activity results in muscular function defects compromising parasite sur-vival in vivo. As whole-body knockouts of mouse STK25 are homozygous viable and display no obvious deleterious phenotypes (*18*), SmSTK25 represents an attractive target for therapeutic intervention. Similar cross-examination of genes associated with other phenotypic classes (e.g., tissue edema) may provide insights into the specificity of the various phenotypes observed in this work.

Technological advances have paved the way for large-scale analyses of gene function in protozoan parasites (*19–21*), but such analyses have been lacking for helminth parasites. Our systematic analysis of gene function in schistosomes allowed us to effectively prioritize targets and potential specific inhibitors with activities on worms. Future efforts should further explore the potency and selectivity of not only the compounds our studies have uncovered (Fig. 2, A and B, and table S6) but also larger libraries of compounds with known molecular targets (*22*). However, to mitigate potential issues with host toxicity, it is also worth exploring whether parasite-selective inhibitors

of validated target proteins can be uncovered. Not only does this study enhance our understanding of schistosome biology, but also it provides a new lens to prioritize genes of interest in other medically and agriculturally important parasitic flatworms. Collectively, we anticipate such studies will expedite the discovery of new antihelminthics.

REFERENCES AND NOTES

1. A. Guidi *et al.*, *PLOS Negl. Trop. Dis.* **9**, e0003801 (2015).
2. J. J. Collins 3rd *et al.*, *Nature* **494**, 476–479 (2013).
3. J. J. Collins 3rd, G. R. Wendt, H. Iyer, P. A. Newmark, *eLife* **5**, e12473 (2016).
4. E. J. Pearce, A. S. MacDonald, *Nat. Rev. Immunol.* **2**, 499–511 (2002).
5. J. Wang, R. Chen, J. J. Collins 3rd, *PLOS Biol.* **17**, e3000254 (2019).
6. M. Buszczak, R. A. Signer, S. J. Morrison, *Cell* **159**, 242–251 (2014).
7. B. Bibo-Verdugo *et al.*, *ACS Infect. Dis.* **5**, 1802–1812 (2019).
8. J. F. Nabhan, F. El-Shehabi, N. Patocka, P. Ribeiro, *Exp. Parasitol.* **117**, 337–347 (2007).
9. D. Mendez *et al.*, *Nucleic Acids Res.* **47** (D1), D930–D940 (2019).
10. L. Rojo-Arreola *et al.*, *PLOS ONE* **9**, e87594 (2014).
11. D. J. Anderson *et al.*, *Cancer Cell* **28**, 653–665 (2015).
12. P. Magnaghi *et al.*, *Nat. Chem. Biol.* **9**, 548–556 (2013).

13. K. Newton *et al.*, *Cell* **134**, 668–678 (2008).
14. D. F. Ceccarelli *et al.*, *J. Biol. Chem.* **286**, 25056–25064 (2011).
15. C. L. C. Poon *et al.*, *Dev. Cell* **47**, 564–575.e5 (2018).
16. C. Preisinger *et al.*, *J. Cell Biol.* **164**, 1009–1020 (2004).
17. G. Wendt *et al.*, *Science* **369**, 1644–1649 (2020).
18. M. Amrutkar *et al.*, *Diabetes* **64**, 2791–2804 (2015).
19. S. Alsford *et al.*, *Genome Res.* **21**, 915–924 (2011).
20. E. Bushell *et al.*, *Cell* **170**, 260–272.e8 (2017).
21. S. M. Sidik *et al.*, *Cell* **166**, 1423–1435.e12 (2016).
22. J. Janes *et al.*, *Proc. Natl. Acad. Sci. U.S.A.* **115**, 10750–10755 (2018).
23. J. Collins, Large-scale RNAi screening uncovers new therapeutic targets in the human parasite Schistosoma mansoni. Dryad (2020); doi:10.5061/dryad.zs7h44j4v.

SUPPLEMENTARY MATERIALS

science.sciencemag.org/content/369/6511/1649/suppl/DC1
Materials and Methods
Figs. S1 to S11
Tables S1 to S10
References (*24–60*)
Movies S1 to S4
MDAR Reproducibility Checklist

View/request a protocol for this paper from *Bio-protocol*.